Pulse Modulators for Ion Recirculator Cells*

T.F. Godlove, L.K. Len, F.M. Mako, FM Technologies, Fairfax, VA 22032
and W.M. Black and K. Sloth, George Mason University, Fairfax, VA 22030

I. INTRODUCTION

Heavy-ion fusion (HIF) continues to be the choice method of inertial fusion energy for a combination of reasons --primarily driver efficiency, beam transport to target, and repetition rate. For more than a decade a group at the Lawrence Berkeley Laboratory (LBL) has explored the use of a multiple-beam induction linear accelerator for the driver. A review of technology development, particularly for a test accelerator called ILSE, has been given by Reginato [1]. Recently, the 5-MeV part of ILSE, dubbed ELISE, has been approved.

In 1989 studies began on the idea of recirculating the linac beams to reduce cost. While a recirculator introduces serious issues, the cost reduction incentive is real. A review of a two-year study, primarily at the Lawrence Livermore National Laboratory (LLNL), has been given by Barnard *et al* [2]. Also, initial technology development for a recirculator at LLNL has been reported by Newton and Kirbie [3].

We report here on a study of circuits for the accelerating modules in a recirculator. Future requirements are challenging: flat-top (or slightly rising) pulses with varying duration; beam currents as high as a kiloampere; a train of 50-100 pulses with instantaneous repetition rate as high as 50 kHz; and high efficiency. An accelerating module providing 200-400 kV to the beam might house 30-100 cores.

Our study uses cores of moderate size--we chose 20.3 cm diameter. The pulsers use tapered pulse-forming networks (PFNs) and provide core reset, 20-µs recovery and variable duration. A novel addition is a separate, 150-kV, 200-A modulator used to simulate a constant-current ion beam, allowing a direct measurement of the cell dynamic impedance and the modulator-to-beam conversion efficiency.

The basic goal of the project is to explore the use of solid-state switches and low-voltage circuits with efficiency and low cost in mind. In this report we describe our circuits and salient results, then offer comments and conclusions.

II. CELL AND CIRCUIT

The cell design, shown in Fig. 1, is conventional. The housing provides for three coax inputs connected to the single-turn conducting wall and is designed for stacking by removing one end wall from each adjacent cell. The core is Metglas** 2605-SC, 10.2 cm ID, 20.3 cm OD, and 5.1 cm wide. It provides 1.94 kV-µs per Tesla magnetic swing. We tried both annealed (before winding) and unannealed cores.

* Supported by DOE Small Business Innovation Research
and in part by Virginia's Center for Innovative Technology.
** Registered trademark of Allied Signal Corporation.

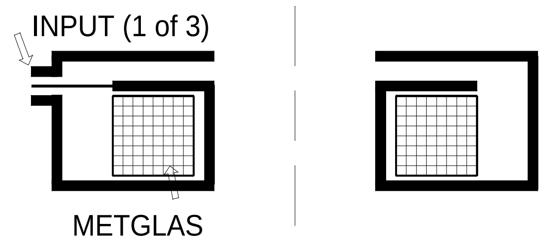

Fig. 1. Model cell. Core O.D. = 20 cm.

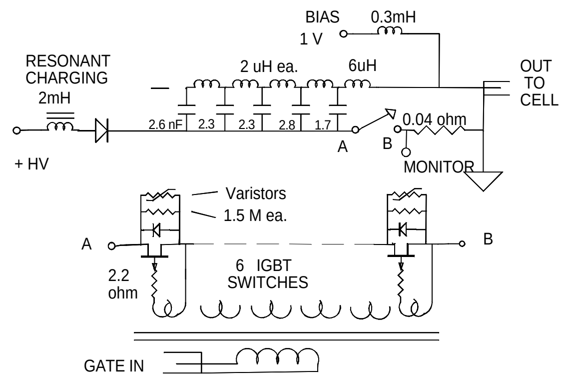

Fig. 2. Cell pulser, one of three for each cell.

Figure 2 shows our 0.4-µs pulser circuit, one of three for each cell. We also built a 0.9-µs, 8-section network. As shown, it uses a 3.5 kV power supply and diode-resonant charging. The charging current partially resets the core magnetization and is supplemented by a small dc current (<6 A) connected through a 0.3-mH isolating inductor. A non inductive, 40-mΩ resistor monitors the pulse current.

Transient suppression, not shown in Fig. 2, is included from A to B. For some tests, we connected the switch assembly between the network and the cell. In this case we lose the charging current reset. More dc bias current, up to about 12 A, is then required.

An important alternative circuit, command resonant charging, is discussed in the next section.

The PFN values are adjusted to give the best flat-top pulse taking into account the cell inductance, transient magnetization current, transient eddy current losses, core saturation, and the time-dependent switch resistance. While the well known design code PSPICE was extensively used and gave excellent agreement with a resistive load, final adjustment of the pulse shape was done empirically.

A principal motivation for the project was the advent of high power solid-state switches, MOSFET and IGBT (insulated-gate bipolar transistor). They provide turn-off capability and can easily recover voltage hold-off in a few μs. We decided early in the project to concentrate on IGBTs because of their higher power rating, in spite of their somewhat slower rise/fall time. Also, they were much lower in cost, although currently the MOSFETS are coming down in price. We used six in series, APT50GF100BN or Int'l Rectifier IRGPC50U or IRGPH50F, rated at 900-1200 V each and up to 200 A peak.

The switch gates are driven using a small pulse transformer with six single-turn secondaries and a six-turn primary driven by a single MOSFET. This method provides the necessary isolation, speed and peak current to the gates. Gate duration is adjusted to coincide with the natural fall of the PFN pulse, resulting in a faster fall time than the IGBT alone provides.

In general the switches only fail due to overvoltage. A varistor is connected in parallel with each switch for fault protection; more on this issue in the next section.

Simulation is accomplished using a separate high-impedance source as shown in Fig. 3. It is a thyratron-switched modulator driving a resistive load on the cell axis. A real beam is a constant-current source. Simulation requires that the voltage added by the cells be small compared to the modulator voltage. The rise time, 0.4 μs, is longer than desired for rise-time simulation but adequate for impedance and efficiency measurements.

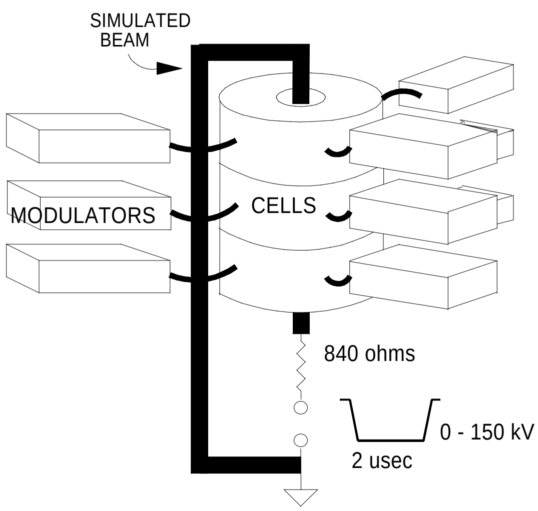

Fig. 3. Simulated beam setup with three cells, each driven by three modulators.

III. RESULTS AND COMMENTS

Figure 4 shows a set of typical waveforms for an annealed core with zero beam current, using the capacitor-grounded circuit and the longer pulse. The four traces show many aspects of circuit behavior. Trace 1 is the PFN voltage on a slow, 0.2 ms, sweep. It shows the 24-μs recovery and voltage remaining after each of two pulses. We ignore the first pulse, since it is based on the supply voltage, 3.5 kV. The voltage then rises to 5 kV, which is the limit of our six switches, and the circuit is triggered again after a delay of 104 μs (the delay is arbitrary from 25 μs to 1 ms, after which the PFN voltage droops).

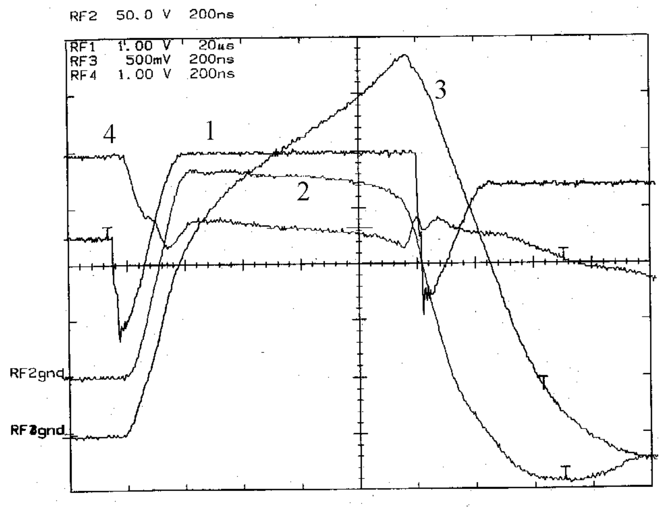

Fig. 4. Waveforms for one cell (1/27/95#1).

Traces 2, 3 and 4 refer to the second pulse. They are the output gap voltage (3.7 kV), current from one pulser (67 A) and PFN voltage, respectively, with a 2-μs sweep. The total current to the cell is 3x67=201 A peak. Trace 2 shows the droop and trace 3 the accelerated current rise during the last 200 ns of the pulse, both due to the onset of core saturation. (The gap voltage is flat at lower supply voltage.) Trace 4 shows, during the first 200 ns, effects of the transient switch resistance. (Note that the PFN is adjusted for trace 2 flatness, not trace 4.) Trace 4 also shows a small inductive transient just after the pulse.

After the second pulse, the PFN voltage rises to an intermediate value, 4.4 kV, a result of the resonant charging method combined with the fact that some energy remains in the PFN. This point is discussed below.

The general behavior shown in Fig. 4 is very similar for the 0.4-μs pulse, and for the alternate circuit.

Variable Duration

The large negative overshoot seen in trace 2 of Fig. 4 is typical of these circuits and leads to an important conclusion. Early in the project we speculated that the pulse duration could be varied in two or three steps by setting the onset of one core pulse to coincide with the fall of another core pulse. In effect the beam would see a longer pulse. This method does not work, in part because of the overshoot, and also because of small transients where the two pulses overlap. However, the simpler alternative method works very well, as follows.

The pulse duration is varied by designing the PFN for the longest pulse and reducing the gate duration for shorter pulses. While this may be obvious given solid-state switches, we were concerned about switch burnout from the transient always present when large currents are turned off in inductive circuits.

We find that the transient is not serious. For long pulses, where the switch is opened at the end of the pulse, the current and remaining energy is adequately small (trace 4 in Fig. 4). As the gate duration is shortened corresponding to higher required beam currents, loading by the beam dominates the circuit and the inductive "spike" is still small. Where efficiency is not an issue (e.g., for ILSE), the question is moot since the duration can be fixed.

Dynamic Impedance

As soon as the beam simulation circuit functioned, we demonstrated an important conclusion: the current supplied by the modulators automatically increases linearly as the simulated beam current is increased. For example, the total peak cell current increased from 114 A to 210 A as the beam current increased from zero to 125 A. At the same time the gap voltage decreased from 2.7 kV to 1.8 kV. We thus found the dynamic impedance, $-dV_{gap}/dI_b$, to be 7.3 Ω for one cell with three PFNs. Three cells yielded 20 Ω, in rough agreement with that expected.

Figure 5 illustrates a problem with our simulation: the rise time of the beam modulator is long (~0.4 µs). The beam drives current into the strongly-coupled core pulsers before they are fully on. This results in the negative transient just before the main pulse and some distortion of the flat top. The distortion varies with the delay of the beam relative to the pulsers. The example shown, and the impedance values above, are for the 0.4-µs PFN, below saturation.

A lower dynamic impedance would reduce the above effect; it would also reduce the possibility of unstable behavior in a real recirculator. For this purpose additional core pulsers can be added. For example, six pulsers could be connected to each cell. The method pursued by the LLNL group, based on discharge of a large capacitor bank, provides a low source impedance but does not easily lend itself to pulse shaping and requires considerably more energy storage.

Efficiency

The efficiency of this cell/circuit combination is relatively good. To quantify this we use a simple, direct method to measure loss: compare the pulse energy delivered to the "beam" ($\tau V_{gap} I_b$, where τ is the duration), with the energy stored in the PFN ($CV_{pfn}^2/2$) minus any energy remaining in the PFN. For reasonable accuracy the method depends on the relatively rectangular pulse provided by the switches and the tapered PFN. At zero beam current the loss measured in this way is primarily core loss, including both magnetization and eddy loss. We found the switch loss is ~8% of the core loss.

Using this method we find the core loss for 0.9 µs fits the curve $W = 50(V_{gap})^{1.8}$ mJ, with V in kV, for the annealed cores up to our present limit, 3.6 kV. From these measurements we calculate a promising efficiency of 72% for a beam current, 250 A, roughly matched to the cell impedance. The unannealed core is considerably more lossy, e.g., at 3.2 kV it is 700 mJ *vs.* 405 mJ for the annealed cores. (At higher gap voltage the pulse shape for the unannealed core has substantial droop.)

For low beam current a significant amount of energy remains in the PFN after each pulse; for high beam current the core loss tends to be small compared to the energy delivered to the beam. The core is basically viewed as a transformer, with little circuit loss other than the transformer itself.

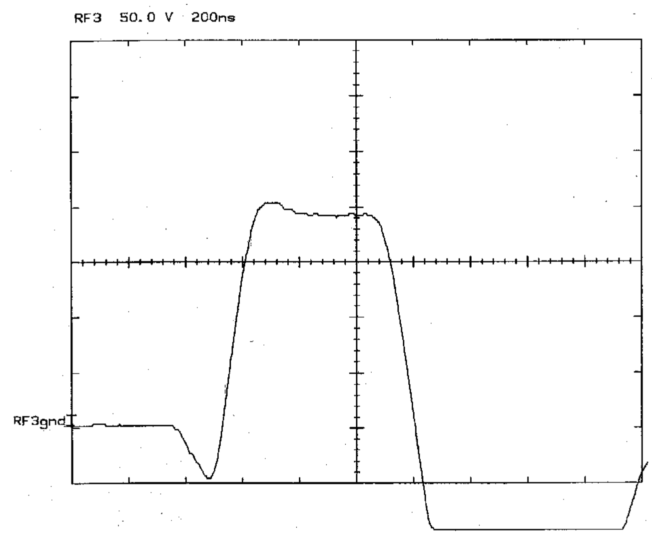

Fig. 5. V_{gap} = 4kV (3 cores), with 96-A beam (11/7/94#1).

Some dc bias reset current, in the 2-3 A range, was always necessary. Near saturation the required bias increased to 5 A for the circuit which provided reset and 10-15 A for the circuit which did not.

Command Charging

Command charging provides more precise control of the PFN voltage. We have used a single IGBT with a 20-µs gate to drive a 1:9 stepup transformer, yielding a secondary pulse of 5 kV. This pulse drives three PFNs directly with the normal 2-mH charging inductors removed. The leakage inductance of the pulse transformer is ideal for the resonance charging inductance. Command charging has an important bonus: the varistors used for fault protection can be chosen to use the most suitable regime of their nonlinear resistance, allowing optimum protection for the solid-state switches.

In summary, we have successfully developed core driving circuits which are relatively efficient, low in cost and whose pulse shape can be precisely tailored. We believe these methods can be extended to higher voltage.

We thank A. Fisher and many members of the LBL and LLNL HIF groups for discussions and assistance.

REFERENCES

[1] L.L. Reginato, Proc. 1993 Part. Accel. Conf., IEEE Cat. 93CH3279-7, 656 (1993); also Proc. Int. Symp. on Heavy Ion Inertial Fusion, Nuovo Cimento 106A, 1593 (1993).

[2] J.J. Bernard, F. Deadrick, A. Friedman, D.P. Grote, L.V. Griffith, H.C. Kirbie, V.K. Neil, M.A. Newton, A.C. Paul, W.M. Sharp, H.D. Shay. R.O. Bangerter, A. Faltens, C.G. Fong, D.L. Judd, E.P. Lee, L.L. Reginato, S.S. Yu, and T.F. Godlove, Phys. Fluids B5, 2698 (1993); also J.J. Barnard *et al*, Nuovo Cimento 106A, 1547 (1993).

[3] M.A. Newton and H.C. Kirbie, Proc. Int. Symp. on Heavy Ion Inertial Fusion. Nuovo Cimento 106A, 1575 (1993).